



Application of 3D Printed Porous Copper Anode in Microbial Fuel Cells

Bin Bian^{1,2}, Chunguang Wang^{1,2*}, Mingjun Hu², Zhaoliang Yang², Xiaobing Cai², Dai Shi² and Jun Yang^{2*}

¹ Xi'an Modern Chemistry Research Institute, Xi'an, China, ² Department of Mechanical and Materials Engineering, Western University, London, ON, Canada

In this study, 3D printing technique was utilized to fabricate three-dimensional porous electrodes for microbial fuel cells with UV curable resin, followed by copper electroless plating. A maximum voltage of 62.9 ± 2.5 mV and a power density of 6.45 ± 0.5 mWm⁻² were achieved for MFCs with 3D printed porous copper (3D-PPC) anodes, which were 8.3- and 12.3-fold higher than copper mesh electrodes, respectively. This illustrated the great advantage of 3D porous anodes in MFCs compared to flat anode structures. Besides, the biocompatibility of the copper anode with *Shewanella oneidensis* MR-1 was examined by comparing with carbon cloth, which produced a 3-fold larger maximum voltage and a ~10-fold higher power density vs. 3D-PPC anodes and thus indicated the possible copper corrosion during MFC operation. ICP-MS analysis of MFC solution revealed the high concentration of 732 ± 27.1 μg/L copper ions detected in the MFC effluent. This result, coupled with EDX showing the lower copper content on the 3D-PPC anode surface after >15 days of MFC operation, confirmed the copper dissolving behavior in MFC. MR-1 biofilm formation under copper suppression was finally characterized by SEM and less biofilm was observed on copper anodes, illustrating their poor biocompatibility, even though 3D printing technology and porous structures were quite promising for future scale-up.

Keywords: 3D printing, 3D porous copper electrode, microbial fuel cell, copper corrosion, *Shewanella oneidensis* MR-1, biocompatibility

OPEN ACCESS

Edited by:

Adrián Escapa,
Universidad de León, Spain

Reviewed by:

Uwe Schröder,
Technische Universität Braunschweig,
Germany

Sunil A. Patil,
Indian Institute of Science Education
and Research Mohali, India

*Correspondence:

Chunguang Wang
king19850723@163.com
Jun Yang
jyang@eng.uwo.ca

Specialty section:

This article was submitted to
Bioenergy and Biofuels,
a section of the journal
Frontiers in Energy Research

Received: 04 April 2018

Accepted: 30 May 2018

Published: 15 June 2018

Citation:

Bian B, Wang C, Hu M, Yang Z, Cai X,
Shi D and Yang J (2018) Application of
3D Printed Porous Copper Anode in
Microbial Fuel Cells.
Front. Energy Res. 6:50.
doi: 10.3389/fenrg.2018.00050

INTRODUCTION

Microbial fuel cells (MFCs) are promising devices in wastewater treatment industry, which generate bioelectricity through degradation of organic matters with the catalysis of exoelectrogenic microorganisms (Logan, 2009; Logan and Rabaey, 2012). Bacteria on the anode oxidize organic compounds anaerobically and produce electrons, protons and CO₂. Electrons are then transferred through the external circuit from anode to cathode, on which electrons couple with protons (diffused from the anode) and oxygen (or other electron acceptors) to form water.

Anode, serving as the bacteria carrier in MFC, plays a significant role in bacterial adhesion and electron transfer from microbes to electrodes. Various materials and strategies have been utilized to improve MFC anode properties, including metal and non-metal materials with/without modification. (Rosenbaum et al., 2007; Rinaldi et al., 2008; Ghasemi et al., 2013) Carbon anodes

[especially materials with high porosity and large surface area, such as carbon cloth (Yuan et al., 2010), carbon fiber brush (Logan et al., 2007; Wang et al., 2011; Wei et al., 2011), PPy-CNTs (Zou et al., 2008), CNT/PANI (Nourbakhsh et al., 2017), graphene (Xie et al., 2012; Wang H. et al., 2013)] are widely used in MFCs due to their excellent stability and biocompatibility. However, 3D porous electrodes recently reported had either large ($>500\ \mu\text{m}$) (Xie et al., 2011; Yong et al., 2012) or small ($<10\ \mu\text{m}$) (He et al., 2012) pore sizes that could hardly be tuned. As the performances of MFC anodes are significantly affected by anode materials and matrix structures, of which a too large or too small porous structure may not be ideal for bacteria growth (Nguyen et al., 2013), it would be meaningful if we could fabricate anodes with both good conductivity and precisely controlled pore sizes.

Apart from carbon materials, metal electrodes, such as 3D stainless steel structures, have been reported to have an equal or even better performance compared with carbon materials (Pocaznoi et al., 2012; Guo et al., 2014, 2015; Ketep et al., 2014; Baudler et al., 2015). However, three-dimensional (3D) metal porous anode with fine and single pore size have been seldom studied in MFC. 3D printing recently draws lots of attention as a unique fabrication technique, allowing one to precisely create sophisticated and low-cost structures and devices (Geissler and Xia, 2004). Metallic structures, especially ultra-light cellular metals with controllable and fine pore sizes and excellent electrical properties, have been widely developed via 3D printing according to people's specific requirements (Wang X. et al., 2013; Wang et al., 2014). Recently, Bian et al. (2018) developed a carbonaceous electrode preparation technique with precisely controllable pore structures and excellent biocompatibility via 3D printing, demonstrating the great potential of printing technique in MFC application and scale-up. However, it's usually energy-intensive to fabricate carbonaceous electrodes, since it requires high temperatures for material carbonization. Considering 3D printed matrixes could also be easily metalized through polymer surface modification with copper (Zhang et al., 2016, 2017) and highly conductive copper anode in MFC with mixed cultures exhibited ambiguous properties (Zhu and Logan, 2014; Baudler et al., 2015, 2017), it would be of great interest to test whether 3D printed copper anode could enhance the bioelectricity generation and biofilm growth of pure culture in microbial fuel cells.

In this study, 3D printed porous copper (3D-PPC) electrode with precisely controlled porous structures was fabricated via 3D printing and copper electroless plating, to function as an anode in MFC. The electrochemical performances of MFCs with 3D-PPC anodes were examined and compared with copper mesh and carbon cloth anodes, to check the effects of 3D porous structures and copper coating on bacterial growth. *Shewanella oneidensis MR-1* was chosen as the pure culture inoculum in MFCs in the hope that it could survive on the copper electrode and thus be further used for heavy-metal wastewater treatment, since it was reported to have high tolerance of heavy metals. (Toes et al., 2008; Wu et al., 2010; Zhou et al., 2016; Kimber et al., 2018) Copper ion concentration in media and *S. oneidensis MR-1* biofilm formation on the anodes were also investigated to explain the test results of each MFC

and identify whether copper corrosion happened during MFC operation.

MATERIALS AND METHODS

Fabrication of 3D-PPC Anode

The porous lattice structures (2.75 cm in diameter and 0.5 cm in thickness with a pore size of $500\ \mu\text{m}$) were first designed using Solidworks and then printed out layer-by-layer by a digital-light-processing (DLP) 3D printer with UV curable resin (Asiga). The parameters set for this printing process were reported previously (Bian et al., 2018). The 3D printed structures were sonicated in ethanol for 10 min and washed 3 times with DI water to remove any uncured polymer before being dried in air for 30 min.

As for the copper electroless plating, 3D printed porous samples were first immersed into 2.5 g/L palladium acetate ($\text{Pd}(\text{Ac})_2$) acetone solution for 20 min, during which $\text{Pd}(\text{Ac})_2$ infiltrated the surface of the 3D printed matrixes with the diffusion of acetone and served as activation sites for later copper coating. After being rinsed with DI water, the $\text{Pd}(\text{Ac})_2$ loaded samples were then placed into the copper plating bath for 1 h, which contains a 1:1 mixture of freshly prepared solution A and B. (**Scheme 1**) Solution A consisted of 14g/L $\text{CuSO}_4 \cdot 5\text{H}_2\text{O}$, 20g/L EDTA-2Na, 11g/L NaOH, 20 mg/L 2,2'-dipyridyl, 10 mg/L potassium ferrocyanide and 16 g/L potassium sodium tartrate. Solution B was 16.5 ml/L HCHO in DI water. Anodes made from copper mesh (50×50 , McMaster-Carr) and carbon cloth (Fuel Cells Etc) were designed with the same projected area of $6\ \text{cm}^2$.

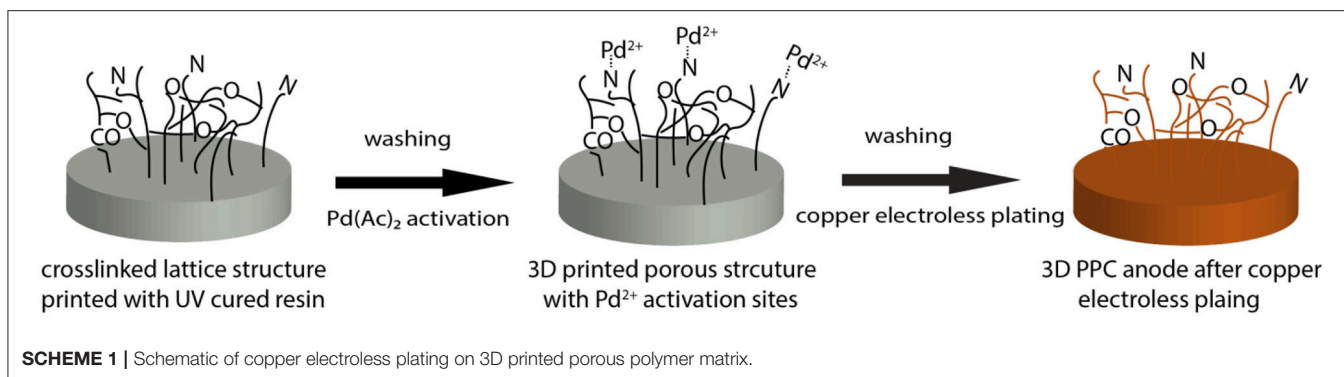
Cultivation and MFC Operation

Shewanella oneidensis MR-1 (wild-type) was chosen as inoculum for MFC operation and cultured aerobically in Tryptic Soy Broth (TSB, BD) for 3 days at 30°C , with shaking at 150 rpm. Bacteria were then centrifuged (5,000 rpm, 6 min) and washed three times in phosphate buffer solution (PBS, Dulbecco's, Sigma) before being adjusted to the desired cell concentration (OD_{600} 0.4). The washed cells were inoculated into MFCs and the media used for *MR-1* tests was the same as the growth media used by Bretschger et al. with 18 mM lactate, vitamins and mineral solution (both from ATCC) (Bretschger et al., 2007).

Single-chamber MFC reactors (4 cm long, 3 cm in diameter, 28 ml volume, Phychemi) were constructed with 3D-PPC, copper mesh and carbon cloth anodes prepared above. All the reactors were run in duplicates, equipped with the air-cathode made from carbon cloth ($7\ \text{cm}^2$, coated with $0.5\ \text{mg}/\text{cm}^2$ Pt/C, Fuel Cells Etc). The spacing between the anode and the cathode was 2 cm and all MFC chambers were sealed by epoxy and autoclaved before use. Cell voltages across a $1,000\ \Omega$ external resistor in the circuit was monitored every 5 min using a high-resolution DAQ device (NI USB 6251 BNC, National Instruments) and the LabVIEW software package (National Instruments).

Characterization

A four-probe method (M2750 Keithley Multimeter) was carried out to measure the sheet resistance of 3D-PPC anode after electroless plating. MFC performances were characterized with linear sweep voltammetry (LSV) (CHI 1200a, CH Instruments



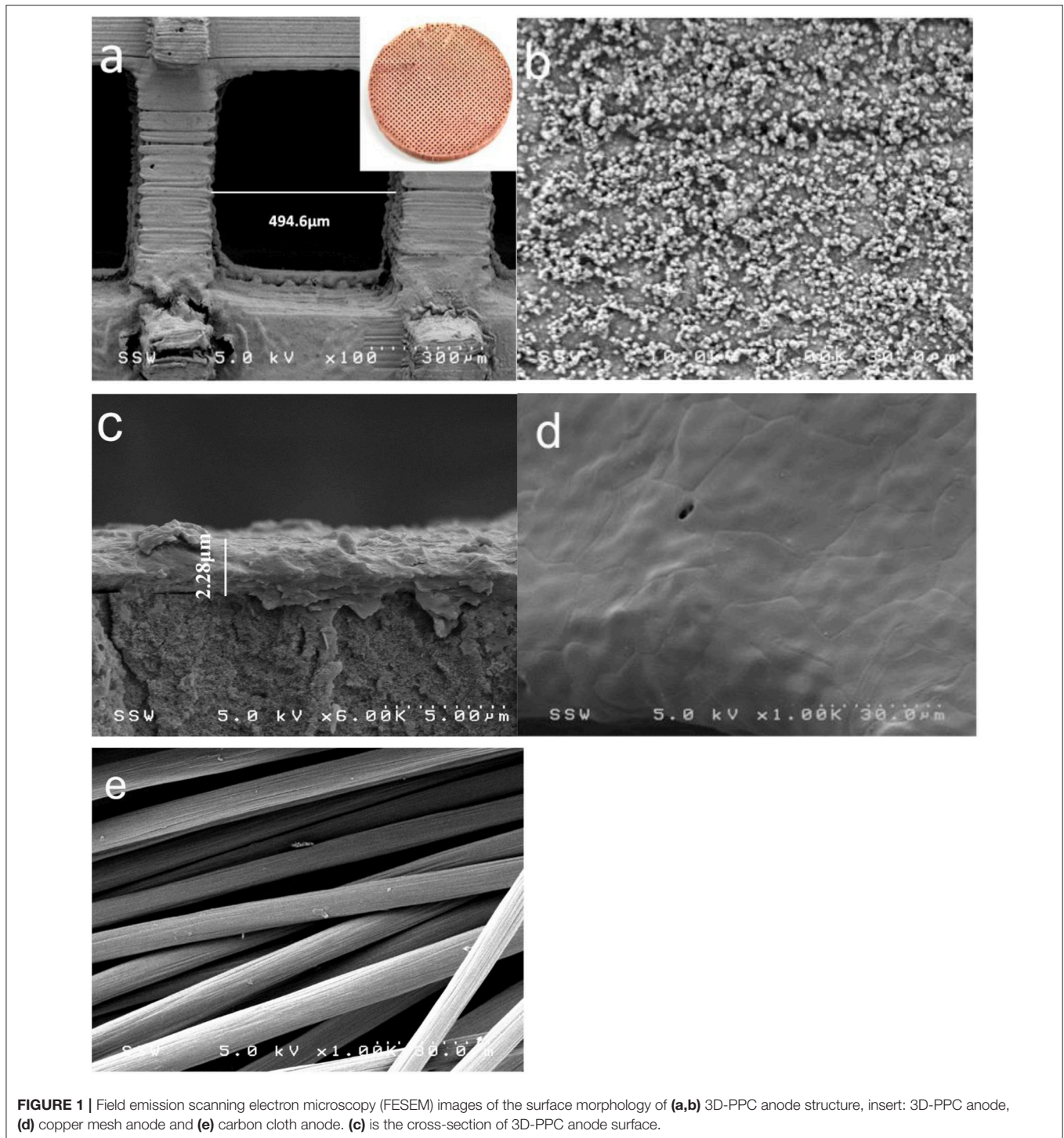
Inc.), at a scanning rate of 0.1 mV s^{-1} from open circuit potential to 0.01 mV . Power densities from each MFC reactor were calculated based on the polarization curves and normalized with the anode projected surface area (6 cm^2). Anode surface morphology was characterized by SEM (S-4500, Hitachi) before and after biofilm formation. Bacterial cells on the anode were first fixed with PBS containing 3% glutaraldehyde overnight at 4°C and then dehydrated in a series of graded ethanol solution before SEM with 60 s gold deposition (Ray et al., 2010). Copper ion concentration in the effluent was detected with inductively coupled plasma mass spectrometry (7700x ICP-MS, Agilent Technologies), to determine whether copper corrosion happened during MFC operation. This detection was coupled with energy-dispersive X-ray (EDX) analysis of copper coating on 3D-PPC anodes before and after MFC operation.

RESULTS AND DISCUSSION

Before the MFC operation, the anode materials were characterized by SEM. As shown in **Figure 1c**, the 3D-PPC anode surface, covered with a thin copper layer ($\sim 2.28 \mu\text{m}$) after 1 h electroless deposition, exhibited excellent electrical conductivity with a surface sheet resistance of $0.017 \Omega/\text{sq}$. Based on the equation of $\rho = R_s \times t$ (in which ρ is the bulk resistivity of materials, R_s is the sheet resistance and t is the thickness of the coating layer), the bulk resistivity ρ of the as-deposited copper layer is calculated to be $3.88 \times 10^{-8} \Omega \text{ m}$, which was 2.25 times higher compared to the normal bulk copper and much better compared to the carbon cloth anode (Oh et al., 2006). Apart from the excellent conductivity of 3D-PPC anode, **Figure 1a** illustrated that the pore size of the 3D printed structures was precisely controlled even after copper electroless plating, with a printing error less than 1.1%. The high-resolution SEM image (as shown in **Figure 1b**) indicated that copper nanoparticles were uniformly distributed on the surface of 3D-PPC anode in addition to the macro porous structures, forming high density of secondary pores after electroless plating. These copper nanoparticles efficiently increased the porosity of 3D-PPC anodes (92–95%) and activation sites, which would probably enable more bacterial adhesion in MFC. On the contrary, the surface of copper mesh turned out to be quite smooth. Pores

or wrinkles that could prompt bacterial growth and adhesion were seldom observed (**Figure 1d**). As for the carbon cloth anode, the total porosity of 80% was achieved according to the manufacturer. However, the surface of carbon fibers was glossy as illustrated in **Figure 1e**, which would probably limit the high power output of MFC with carbon cloth.

All MFCs with different anode materials were batch-fed for more than 15 days, but the performances of each MFC varied in the first several cycles. MFCs with 3D-PPC anodes and copper mesh anodes immediately generated high maximum voltages after being connected to the external resistors, which was consistent with the results obtained by Zhu and Logan (2014). The maximum voltage produced during the 3-day first cycle was $224.5 \pm 32.4 \text{ mV}$ for 3D-PPC anodes compared to $179.1 \pm 22.8 \text{ mV}$ from copper mesh anodes. This observation was abnormal since *Shewanella MR-1* has never been reported to achieve such high maximum voltages in previous literature (Bretschger et al., 2007; Watson and Logan, 2010; Nourbakhsh et al., 2017; Bian et al., 2018). The peak voltages from copper anodes dropped dramatically to $95.2 \pm 5.9 \text{ mV}$ and $45.2 \pm 9.4 \text{ mV}$, respectively, in the second cycle (**Figure 2**). After about 10 cycles, the maximum voltages of MFCs with 3D-PPC anode stabilized at about $62.9 \pm 2.5 \text{ mV}$ while only $7.6 \pm 0.25 \text{ mV}$ was achieved by copper mesh anode over successive cycles. MFCs with carbon cloth anodes, however, initially generated very low voltages when being inoculated with *Shewanella MR-1* (**Figure 2**). The maximum voltage climbed to over 190 mV after 15 cycles and stayed at $188.5 \pm 2.7 \text{ mV}$ afterward. The peak voltages during the MFC operation showed clearly different trends of electricity production between copper anodes and carbon cloth, which indicated the high possibility of copper corrosion from copper anode surface at the beginning of the experiment. In order to identify whether microbes are involved in the voltage production, a control experiment without any inoculum was carried out and 66.5% lower maximum voltage was produced by 3D-PPC anode ($75.1 \pm 3.8 \text{ mV}$) in abiotic conditions as shown in Figure S1. The voltage decreased to less than 10 mV after 7 batches compared to $62.9 \pm 2.5 \text{ mV}$ by *S. oneidensis*-driven MFCs, clearly showing voltages produced in MFCs with copper anodes and *S. oneidensis* were far more than that just from copper corrosion. Also, one important detail we have to point out is that 3D-PPC anode obtained much higher



peak voltage after stabilization, compared to the copper mesh anode. The maximum voltage of 62.9 ± 2.5 mV produced was about 8.3 times larger than that produced by copper mesh anodes and 20 times larger than what has been reported by Zhu and Logan (2014), which demonstrated the superior property of 3D printed porous lattice architecture to boost the power output of MFC.

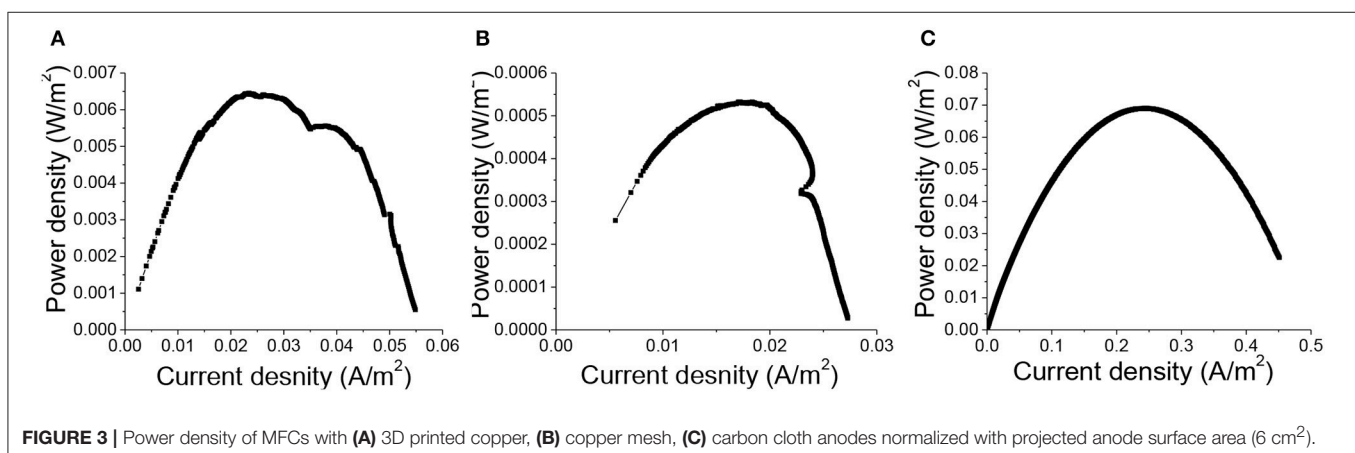
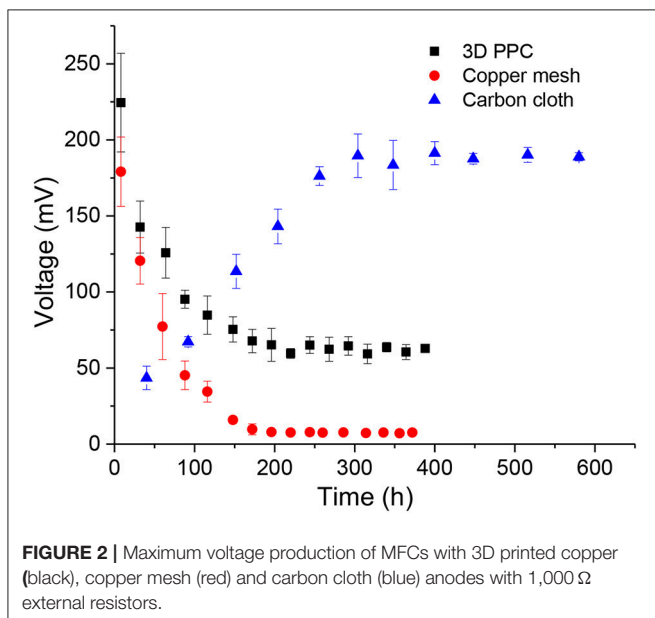
Polarization curves plotting current as a function of voltage were measured when the maximum voltages generated by all MFCs were repeatable over cycles, to evaluate the influence of 3D printed porous structures on the anodic electrochemical behavior of *MR-1* cells fed with lactate. Dual-electrode mode was adopted in the polarization curve measurement, with the three different types of anode materials serving as the working electrodes

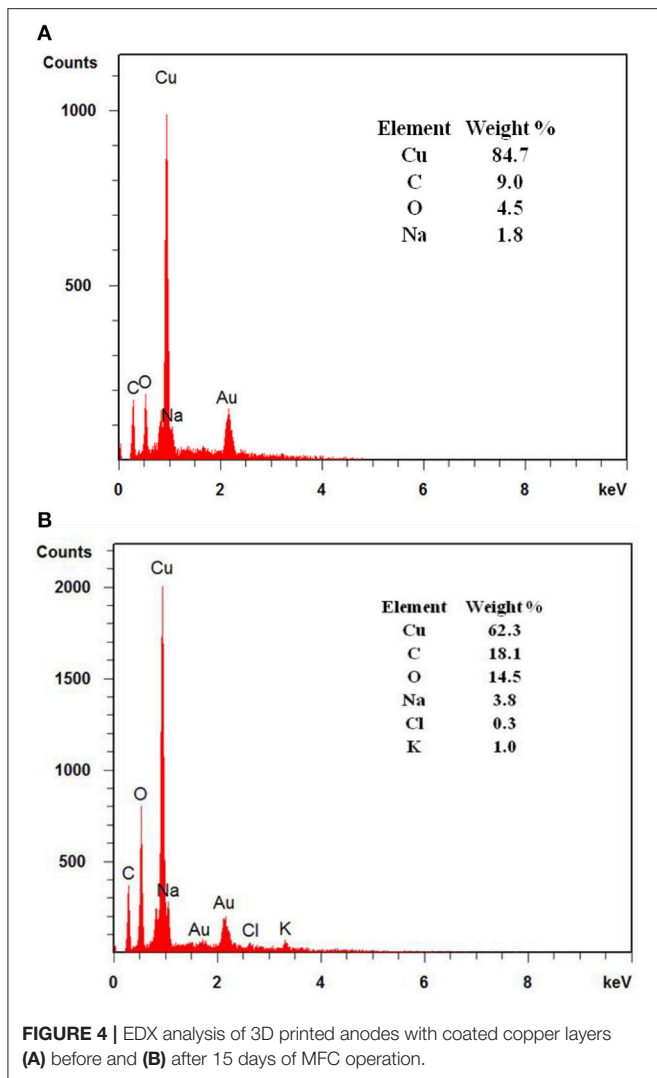
and air-cathodes as the reference and counter electrodes. The maximum power density generated by MFCs with carbon cloth anodes was $69.0 \pm 4.7 \text{ mWm}^{-2}$, compared to $6.5 \pm 0.5 \text{ mWm}^{-2}$ for the 3D printed copper anodes and $0.53 \pm 0.04 \text{ mWm}^{-2}$ for the copper mesh anodes (Figure 3). This result further supported our suspicion that the possible copper corrosion inhibited the growth of *MR-1* and led to the inferior performance of MFCs with copper anodes. However, the power density from 3D-PPC anode was again far higher than that from copper mesh anode, which could be attributed to the higher porosity (92–95% vs. 65–80% for copper mesh), enhanced bacterial colonization and the increased number of active sites when copper nanoparticles were introduced onto the 3D-PPC anode surface. (Gawande et al., 2016) When we compared our data to the power output ($2 \pm 0.3 \text{ mWm}^{-2}$) reported by Zhu et al. with mixed cultures (Zhu and Logan, 2014), it was obvious that 3D-PPC anode could improve the power generation of MFC as it was more than 3 times higher,

considering the commonly low coulombic efficiency of *MR-1* MFCs (Newton et al., 2009).

Though 3D-PPC anodes exhibited higher surface area, both of these two copper anodes were suspected to be corroded during MFC operation, which led to the solution of copper ions in MFC media. In order to check the copper content in the media and on the surface of 3D-PPC anode, ICP-MS and EDX analysis were conducted to clarify the doubts above. For ICP-MS analysis, 2 ml effluent was taken from the MFC chambers with 3D-PPC anodes after 12 and 24 h media feeding, respectively, during the first several cycles. After filtration through $0.2 \mu\text{m}$ filter, the solution was diluted 10 times before being sent for ICP-MS analysis. An average of $732 \pm 27.1 \mu\text{g/L}$ copper ions were detected in the media after 12 h feeding while for the 24 h solution the concentration of copper ions increased to $878 \pm 43.4 \mu\text{g/L}$ (vs. $81.56 \pm 0.25 \mu\text{g/L}$ from copper mesh anode). As there were no copper ions in the feeding media except for the very minimum amount in the mineral solution ($< 30 \mu\text{g/L}$), the copper ions detected came from nowhere but the 3D-PPC anodes. This observation is within the range of copper concentration obtained by Zhu and Logan (2014), however, is completely different from studies by Baudler et al since no metal ions were detected in the effluent of their MFC chambers (Baudler et al., 2015). This could be probably attributed to the anode potential (-0.2 V vs. Ag/AgCl) set in studies by Baudler et al, which was significantly lower than the copper oxidation potential to prevent the metal corrosion (Baudler et al., 2015, 2017). Nevertheless, in our case, the anode potential was never set (due to the lack of proper equipment), resulting in relatively high anode potential in MFCs and dissolving copper ions from the very beginning.

Apart from ICP-MS, EDX analysis of the 3D-PPC anode was also done after more than 15 days of MFC operation (Figure 4). The samples were carefully washed with ethanol and dried before test. The EDX spectrum recorded for the 3D-PPC anode before MFC experiment exhibited a very strong signal of copper with a weight percentage of 84.7%, indicating the excellent copper coverage on the 3D printed polymer matrix before MFC construction. Nevertheless, only 62.3 wt% of copper was detected on the surface of 3D-PPC anode after MFC operation. The copper corrosion on the porous anode surface during MFC operation





was now almost demonstrated here with these analyses. Wu et al. (2010) studied the response of *Shewanella oneidensis* MR-1 to heavy metals Ti/Cu nanoparticles and found 360 $\mu\text{g/L}$ copper ions could inhibit $11 \pm 2\%$ MR-1 growth and 1.8%-Cu doped TiO_2 (360 $\mu\text{g Cu/L}$) nanoparticles kills $15 \pm 8\%$ cells, even though TiO_2 didn't show significant bacterial suppression effects. However, Toes et al. (2008) discovered that the expression of certain proteins, such as copA and cusA, would be enhanced under copper stress. *Shewanella oneidensis* was even found to be able to reduce copper ions into Cu nanoparticles anaerobically in highly-concentrated copper media (Zhou et al., 2016; Kimber et al., 2018). It would be very difficult to conclude that growth of *Shewanella oneidensis* MR-1 was suppressed in MFC with copper ions in this experiment unless clear SEM images of poor bacterial adhesion on copper anode surface are presented.

In order to investigate the impacts of soluble copper on bacterial growth on MFC anode surface, FESEM was used to observe the biofilm formation on the MFC anodes after 15 days of MFC operation. We found that the biofilm grown on the

carbon cloth anode was the thickest among all three different types of anodes (Figure 5). Layers of MR-1 biofilm were formed on the surface of carbon cloth anode, illustrating the better biocompatibility of carbon materials. This also explains the much better performance of MFCs with carbon cloth anodes. However, when we look at the bacterial adhesion on copper anodes, no thick biofilm was found on electrode surface like carbon cloth and copper-based MFC anodes reported by Baudler et al. (2015, 2017). The huge difference of biofilm thickness between 3D-PPC anodes we observed and copper anode reported by Baudler et al. (Baudler et al., 2015, 2017) could be probably attributed to the different bacterial cultures as MFC inoculum. One reason accounting for the rare colonization of *S. oneidensis* cells on copper anodes in this study is that *Shewanella oneidensis* was reported to survive mainly as planktonic cells in MFC chambers (Lanthier et al., 2008). This is totally different from the *Geobacter* species which usually exhibit high biofilm thickness on MFC anode surface (Ren et al., 2008). Since mature and thicker biofilms usually possess higher resistance to antibiotics (Stewart, 1994; Mah and O'toole, 2001; Ito et al., 2009) and mixed cultures have been demonstrated to have varying performances under copper suppression (Dell'amico et al., 2008; He et al., 2010), *Geobacter*-dominated thick biofilm is believed to have the better tolerance against copper and receive interacting supports between different bacterial species, which is probably another reason for the excellent performance of MFCs with copper-based anodes in Baulder et al experiment (Baudler et al., 2015, 2017). However, the suppression effect of copper ions in media on MR-1 cell growth agreed with the results obtained by Zhu and Logan (2014) using mixed cultures as inoculum, which indicates the copper corrosion at high anode potential to be the root cause for inferior MFC performances in this study.

Even though growth of *S. oneidensis* underwent the copper suppression, we could still see the larger number of MR-1 cells and higher cell density immobilized on the 3D-PPC anodes compared to those on copper mesh anodes. MR-1 cells and extracellular polymeric substances (EPS) were found growing and connecting to each other across the pores on the internal anode surface (Figure 5a). Higher-resolution SEM images clearly exhibited bacterial cells on the 3D-PPC anode, however, less copper nanoparticles were found after 15 days MFC operation and copper corrosion. On the contrary, bacterial biofilm could be rarely found on the copper mesh anodes except for some isolated bacterial cells (Figure 5c). As the power output of MFCs mainly depends on the electron transfer between anodes and bacterial cells, we could hardly expect any higher maximum voltage and power density from MFCs with copper mesh anodes. Thus, 3D-PPC anode exhibited much superior performances than copper mesh anode in MFC, even though copper corrosion prevented MR-1 cells from intensively adhering onto the anode surface.

CONCLUSION

In this study, 3D printing technology was successfully utilized to fabricate the 3D architecture with controllable pore sizes,

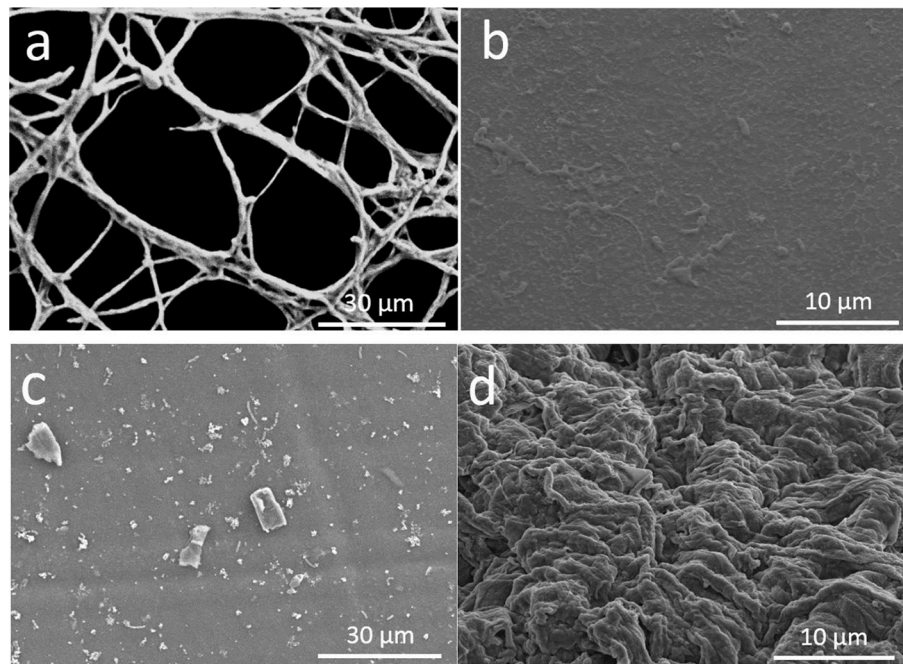


FIGURE 5 | FESEM images of *Shewanella* MR-1 biofilms formed on MFC anodes after 15 days of operation. **(a)** internal pore surface of 3D printed anodes, **(b)** *S. oneidensis* MR-1 cells on 3D PPC anode at higher resolution, **(c)** surface of copper mesh, and **(d)** carbon cloth surface.

followed by copper electroless plating. The performance of this 3D-PPC anodes in MFC was demonstrated to be much superior to that of copper mesh anodes, which was attributed to the higher porosity of 3D-PPC anode with more bacterial adhesion and indicated the great potential of 3D printing technology in various electrode preparation. Besides, the toxicity and suppression of copper ions to pure *Shewanella oneidensis* MR-1 culture in MFCs were confirmed in this study, which inhibited the further enhancement of MFC performances. Novel plating technique of different metals should be thus developed to produce biocompatible electrodes, or low anode potential should be set for the 3D-PPC anodes in MFCs, if we hope to integrate 3D printing technology with bio-electrochemistry for future large-scale waste stream treatment.

AUTHOR CONTRIBUTIONS

BB conducted the experiment and wrote the draft. All the authors played active roles in analysing the results and finalizing the manuscript. JY is the supervisor of BB.

REFERENCES

- Baudler, A., Langner, M., Rohr, C., Greiner, A., and Schröder, U. (2017). Metal-polymer hybrid architectures as novel anode platform for microbial electrochemical technologies. *ChemSusChem* 10, 253–257. doi: 10.1002/cssc.201600814
- Baudler, A., Schmidt, I., Langner, M., Greiner, A., and Schroder, U. (2015). Does it have to be carbon? Metal anodes in microbial fuel cells and

FUNDING

The authors are grateful for financial support from Natural Science and Engineering Research Council of Canada (NSERC), the Canada Foundation for Innovation (CFI) and Research Accelerator Grant of The University of Western Ontario.

ACKNOWLEDGMENTS

The authors are grateful for kind support from Mr Junfeng Xiao in department of Mechanical and Materials Engineering, UWO. We also thank Mr. Brad Kobe for his assistance in SEM characterization.

SUPPLEMENTARY MATERIAL

The Supplementary Material for this article can be found online at: <https://www.frontiersin.org/articles/10.3389/fenrg.2018.00050/full#supplementary-material>

- related bioelectrochemical systems. *Energy Environ. Sci.* 8, 2048–2055. doi: 10.1039/C5EE00866B
- Bian, B., Shi, D., Cai, X. B., Hu, M. J., Guo, Q. Q., Zhang, C. H., et al. (2018). 3D printed porous carbon anode for enhanced power generation in microbial fuel cell. *Nano Energy* 44, 174–180. doi: 10.1016/j.nanoen.2017.11.070
- Bretschger, O., Obraztsova, A., Sturm, C. A., Chang, I. S., Gorby, Y. A., Reed, S. B., et al. (2007). Current production and metal oxide reduction by

- Shewanella oneidensis* MR-1 wild type and mutants. *Appl. Environ. Microbiol.* 73, 7003–7012. doi: 10.1128/AEM.01087-07
- Dell'Amico, E., Mazzocchi, M., Cavalca, L., Allievi, L., and Andreoni, V. (2008). Assessment of bacterial community structure in a long-term copper-polluted ex-vineyard soil. *Microbiol. Res.* 163, 671–683. doi: 10.1016/j.micres.2006.09.003
- Gawande, M. B., Goswami, A., Felpin, F. X., Asefa, T., Huang, X. X., Silva, R., et al. (2016). Cu and Cu-based nanoparticles: synthesis and applications in review catalysis. *Chem. Rev.* 116, 3722–3811. doi: 10.1021/acs.chemrev.5b00482
- Geissler, M., and Xia, Y. N. (2004). Patterning: principles and some new developments. *Adv. Mater.* 16, 1249–1269. doi: 10.1002/adma.200400835
- Ghasemi, M., Daud, W. R. W., Hassan, S. H. A., Oh, S. E., Ismail, M., Rahimnejad, M., et al. (2013). Nano-structured carbon as electrode material in microbial fuel cells: a comprehensive review. *J. Alloys Compd.* 580, 245–255. doi: 10.1016/j.jallcom.2013.05.094
- Guo, K., Donose, B. C., Soeriyadi, A. H., PrévotEAU, A., Patil, S. A., Freguia, S., et al. (2014). Flame oxidation of stainless steel felt enhances anodic biofilm formation and current output in bioelectrochemical systems. *Environ. Sci. Technol.* 48, 7151–7156. doi: 10.1021/es500720g
- Guo, K., Soeriyadi, A. H., Feng, H. J., PrevotEAU, A., Patil, S. A., Gooding, J. J., et al. (2015). Heat-treated stainless steel felt as scalable anode material for bioelectrochemical systems. *Bioresour. Technol.* 195, 46–50. doi: 10.1016/j.biortech.2015.06.060
- He, L. Y., Zhang, Y. F., Ma, H. Y., Su, L. N., Chen, Z. J., Wang, Q. Y., et al. (2010). Characterization of copper-resistant bacteria and assessment of bacterial communities in rhizosphere soils of copper-tolerant plants. *Appl. Soil Ecol.* 44, 49–55. doi: 10.1016/j.apsoil.2009.09.004
- He, Z., Liu, J., Qiao, Y., Li, C. M., and Tan, T. T. (2012). Architecture engineering of hierarchically porous chitosan/vacuum-stripped graphene scaffold as bioanode for high performance microbial fuel cell. *Nano Lett.* 12, 4738–4741. doi: 10.1021/nl302175j
- Ito, A., Taniuchi, A., May, T., Kawata, K., and Okabe, S. (2009). Increased antibiotic resistance of *Escherichia coli* in mature biofilms. *Appl. Environ. Microbiol.* 75, 4093–4100. doi: 10.1128/AEM.02949-08
- Ketep, S. F., Bergel, A., Calmet, A., and Erable, B. (2014). Stainless steel foam increases the current produced by microbial bioanodes in bioelectrochemical systems. *Energy Environ. Sci.* 7, 1633–1637. doi: 10.1039/C3EE44114H
- Kimber, R. L., Lewis, E. A., Parmeggiani, F., Smith, K., Bagshaw, H., Starborg, T., et al. (2018). Biosynthesis and characterization of copper nanoparticles using *Shewanella oneidensis*: application for click chemistry. *Small* 14:1703145. doi: 10.1002/smll.201703145
- Lanthier, M., Gregory, K. B., and Lovley, D. R. (2008). Growth with high planktonic biomass in *Shewanella oneidensis* fuel cells. *FEMS Microbiol. Lett.* 278, 29–35. doi: 10.1111/j.1574-6968.2007.00964.x
- Logan, B., Cheng, S., Watson, V., and Estadt, G. (2007). Graphite fiber brush anodes for increased power production in air-cathode microbial fuel cells. *Environ. Sci. Technol.* 41, 3341–3346. doi: 10.1021/es062644y
- Logan, B. E. (2009). Exoelectrogenic bacteria that power microbial fuel cells. *Nat. Rev. Microbiol.* 7, 375–381. doi: 10.1038/nrmicro2113
- Logan, B. E., and Rabaey, K. (2012). Conversion of wastes into bioelectricity and chemicals by using microbial electrochemical technologies. *Science* 337, 686–690. doi: 10.1126/science.1217412
- Mah, T. F., and O'Toole, G. A. (2001). Mechanisms of biofilm resistance to antimicrobial agents. *Trends Microbiol.* 9, 34–39. doi: 10.1016/S0966-842X(00)01913-2
- Newton, G. J., Mori, S., Nakamura, R., Hashimoto, K., and Watanabe, K. (2009). Analyses of current-generating mechanisms of *Shewanella loihica* PV-4 and *Shewanella oneidensis* MR-1 in microbial fuel cells. *Appl. Environ. Microbiol.* 75, 7674–7681. doi: 10.1128/AEM.01142-09
- Nguyen, T. H., Yu, Y. Y., Wang, X., Wang, J. Y., and Song, H. (2013). A 3D mesoporous polysulfone-carbon nanotube anode for enhanced bioelectricity output in microbial fuel cells. *Chem. Commun.* 49, 10754–10756. doi: 10.1039/c3cc45775c
- Nourbakhsh, F., Mohsennia, M., and Pazouki, M. (2017). Nickel oxide/carbon nanotube/polyaniline nanocomposite as bifunctional anode catalyst for high-performance *Shewanella*-based dual-chamber microbial fuel cell. *Bioprocess Biosyst. Eng.* 40, 1669–1677. doi: 10.1007/s00449-017-1822-y
- Oh, H. J., Lee, J. H., Ahn, H. J., Jeong, Y., Kim, Y. J., and Chi, C. S. (2006). Nanoporous activated carbon cloth for capacitive deionization of aqueous solution. *Thin Solid Films* 515, 220–225. doi: 10.1016/j.tsf.2005.12.146
- Pocaznoi, D., Calmet, A., Etcheverry, L., Erable, B., and Bergel, A. (2012). Stainless steel is a promising electrode material for anodes of microbial fuel cells. *Energy Environ. Sci.* 5, 9645–9652. doi: 10.1039/c2ee22429a
- Ray, R., Lizewski, S., Fitzgerald, L. A., Little, B., and Ringeisen, B. R. (2010). Methods for imaging *Shewanella oneidensis* MR-1 nanofilaments. *J. Microbiol. Methods* 82, 187–191. doi: 10.1016/j.mimet.2010.05.011
- Ren, Z., Steinberg, L. M., and Regan, J. M. (2008). Electricity production and microbial biofilm characterization in cellulose-fed microbial fuel cells. *Water Sci. Technol.* 58, 617–622. doi: 10.2166/wst.2008.431
- Rinaldi, A., Mecheri, B., Garavaglia, V., Licoccia, S., Di Nardo, P., and Traversa, E. (2008). Engineering materials and biology to boost performance of microbial fuel cells: a critical review. *Energy Environ. Sci.* 1, 417–429. doi: 10.1039/b806498a
- Rosenbaum, M., Zhao, F., Quaa, M., Wulff, H., Schroder, U., and Scholz, F. (2007). Evaluation of catalytic properties of tungsten carbide for the anode of microbial fuel cells. *Appl. Catalysis B Environ.* 74, 261–269. doi: 10.1016/j.apcatb.2007.02.013
- Stewart, P. S. (1994). Biofilm accumulation model that predicts antibiotic resistance of *Pseudomonas aeruginosa* biofilms. *Antimicrob. Agents Chemother.* 38, 1052–1058. doi: 10.1128/AAC.38.5.1052
- Toes, A. C., Daleke, M. H., Kuenen, J. G., and Muyzer, G. (2008). Expression of copA and cusA in *Shewanella* during copper stress. *Microbiology-Sgm* 154, 2709–2718. doi: 10.1099/mic.0.2008/016857-0
- Wang, L., Liang, P., Zhang, J., and Huang, X. (2011). Activity and stability of pyrolyzed iron ethylenediaminetetraacetic acid as cathode catalyst in microbial fuel cells. *Bioresour. Technol.* 102, 5093–5097. doi: 10.1016/j.biortech.2011.01.025
- Wang, H., Wang, G., Ling, Y., Qian, F., Song, Y., Lu, X., et al. (2013). High power density microbial fuel cell with flexible 3D graphene-nickel foam as anode. *Nanoscale* 5, 10283–10290. doi: 10.1039/c3nr03487a
- Wang, X., Cai, X., Guo, Q., Zhang, T., Kobe, B., and Yang, J. (2013). i3DP, a robust 3D printing approach enabling genetic post-printing surface modification. *Chem. Commun.* 49, 10064–10066. doi: 10.1039/c3cc45817b
- Wang, X., Guo, Q., Cai, X., Zhou, S., Kobe, B., and Yang, J. (2014). Initiator-integrated 3D printing enables the formation of complex metallic architectures. *ACS Appl. Mater. Interfaces* 6, 2583–2587. doi: 10.1021/am4050822
- Watson, V. J., and Logan, B. E. (2010). Power production in MFCs inoculated with *Shewanella oneidensis* MR-1 or mixed cultures. *Biotechnol. Bioeng.* 105, 489–498. doi: 10.1002/bit.22556
- Wei, J., Liang, P., and Huang, X. (2011). Recent progress in electrodes for microbial fuel cells. *Bioresour. Technol.* 102, 9335–9344. doi: 10.1016/j.biortech.2011.07.019
- Wu, B., Huang, R., Sahu, M., Feng, X. Y., Biswas, P., and Tang, Y. J. (2010). Bacterial responses to Cu-doped TiO₂ nanoparticles. *Sci. Total Environ.* 408, 1755–1758. doi: 10.1016/j.scitotenv.2009.11.004
- Xie, X., Hu, L., Pasta, M., Wells, G. F., Kong, D., Criddle, C. S., et al. (2011). Three-dimensional carbon nanotube-textile anode for high-performance microbial fuel cells. *Nano Lett.* 11, 291–296. doi: 10.1021/nl103905t
- Xie, X., Yu, G. H., Liu, N., Bao, Z. N., Criddle, C. S., and Cui, Y. (2012). Graphene-sponges as high-performance low-cost anodes for microbial fuel cells. *Energy Environ. Sci.* 5, 6862–6866. doi: 10.1039/c2ee03583a
- Yong, Y. C., Dong, X. C., Chan-Park, M. B., Song, H., and Chen, P. (2012). Macroporous and monolithic anode based on polyaniline hybridized three-dimensional graphene for high-performance microbial fuel cells. *ACS Nano* 6, 2394–2400. doi: 10.1021/nn204656d
- Yuan, Y., Zhou, S. G., and Zhuang, L. (2010). Polypyrrole/carbon black composite as a novel oxygen reduction catalyst for microbial fuel cells. *J. Power Sources* 195, 3490–3493. doi: 10.1016/j.jpowsour.2009.12.026
- Zhang, D. X., Xiao, J. F., Qiu, Y. J., Yang, J., and Guo, Q. Q. (2017). Initiator-integrated 3-D printing of magnetic object for remote controlling application. *IEEE Trans. Magn.* 53, 1–9. doi: 10.1109/TMAG.2017.2666777
- Zhang, N. B., Hu, M. J., Shao, L. M., and Yang, J. (2016). Localization of printed chipless RFID in 3-D space. *IEEE Microw. Wireless Components Lett.* 26, 373–375. doi: 10.1109/LMWC.2016.2549264

- Zhou, N. Q., Tian, L. J., Wang, Y. C., Li, D. B., Li, P. P., Zhang, X., et al. (2016). Extracellular biosynthesis of copper sulfide nanoparticles by *Shewanella oneidensis* MR-1 as a photothermal agent. *Enzyme Microb. Technol.* 95, 230–235. doi: 10.1016/j.enzmictec.2016.04.002
- Zhu, X. P., and Logan, B. E. (2014). Copper anode corrosion affects power generation in microbial fuel cells. *J. Chem. Technol. Biotechnol.* 89, 471–474. doi: 10.1002/jctb.4156
- Zou, Y. J., Xiang, C. L., Yang, L. N., Sun, L. X., Xu, F., and Cao, Z. (2008). A mediatorless microbial fuel cell using polypyrrole coated carbon nanotubes composite as anode material. *Int. J. Hydrogen Energy* 33, 4856–4862. doi: 10.1016/j.ijhydene.2008.06.061

Conflict of Interest Statement: The authors declare that the research was conducted in the absence of any commercial or financial relationships that could be construed as a potential conflict of interest.

Copyright © 2018 Bian, Wang, Hu, Yang, Cai, Shi and Yang. This is an open-access article distributed under the terms of the Creative Commons Attribution License (CC BY). The use, distribution or reproduction in other forums is permitted, provided the original author(s) and the copyright owner are credited and that the original publication in this journal is cited, in accordance with accepted academic practice. No use, distribution or reproduction is permitted which does not comply with these terms.